EPJ manuscript No.
(will be inserted by the editor)

Strange prospects for LHC energies

B. Hippolyte[a] for the ALICE Collaboration[b]

Institut Pluridisciplinaire Hubert Curien, Département de Recherches Subatomiques and Université Louis Pasteur, Strasbourg, FRANCE.

Received: date / Revised version: date

Abstract. Strange quark and hadron production will be studied at the Large Hadron Collider (LHC) energies in order to explore the properties of both pp and heavy-ion collisions. The ALICE experiment will be specifically efficient in the strange sector with the identification of baryons and mesons over a wide range of transverse momentum. Dedicated measurements are proposed for investigating chemical equilibration and bulk properties. Strange particles can also help to probe kinematical regions where hard processes and pQCD dominate. We try to anticipate here several ALICE analyses to be performed as the first Pb–Pb and pp data will be available.

PACS. 25.75.-q describing text of that key – 25.75.Dw describing text of that key

1 Introduction

The ALICE experiment at LHC will be a unique tool for understanding strange quark and hadron productions [1]. In relativistic heavy ion collisions, strange particles are used to probe the chemical equilibration of the cooling Quark Gluon Plasma (QGP) which can be created in such high energy density conditions. The extraction of the transverse momentum (p_T) spectra for identified particles is interesting for distinguishing between different hadronization scenarios in the intermediate p_T range. In elementary hadronic collisions, strange particles can help characterizing the underlying event structure and defining a reference for baryon creation. We present here some of the measurements which will be performed with the ALICE experiment both in Pb–Pb and pp collisions.

In the second section, we discuss the chemical composition analysis resulting from particle spectra and yields in Pb–Pb collisions. Particle identification (PID) capabilities and p_T range for hyperons in ALICE are then summarized. The third section is dedicated to strange baryon/meson ratio as a function of p_T, starting with the importance of this measurement with respect to the validity of coalescence models for A–A collisions. It is then shown that high (i.e. close to unity) baryon/meson ratio at intermediate p_T were already reported in pp collisions, hence justifying the need for a reference measurement at LHC energies.

2 Particle yields and ratios for LHC heavy-ion collisions

Excitation functions of many particle yields in heavy-ion collisions are currently available from the Alternating Gradient Synchrotron energies, through the Super Proton Synchrotron (SPS) ones, up to a Relativistic Heavy Ion Collider (RHIC) top energy of $\sqrt{s} = 200$ GeV [2,3,4,5]. Moreover, centrality dependences were also reported and since smooth behaviours were observed over more than two orders of magnitude in energy, clear guidances are given on what these values might be for the LHC Pb–Pb collisions at $\sqrt{s} = 5.5$ TeV.

If some uncertainties remain for the extrapolations of the total multiplicities and specific absolute yields, the large success of statistical thermal models at SPS and RHIC should provide reliable predictions for most particle ratios [6,7]. In the following paragraph, we discuss observables which, by a deviation from model predictions, may reveal new physics related to QGP characteristics and/or evolution.

2.1 Thermal production and strangeness equilibration

Assuming that particle production in heavy ion collisions, as shown previously at SPS and RHIC [6,7] is described by a thermal source, some statistical observables can be extrapolated up to LHC energies. Indeed, a chemical freeze-out temperature and a finite baryo-chemical potential in the statistical thermal model approach can be obtained at equilibrium using a constant average energy per hadron close to 1 GeV [8] which approximately gives T = 165 MeV and $\mu_B = 1$ MeV at $\sqrt{s} = 5.5$ TeV [9].

[a] *Present address:* hippolyt@in2p3.fr
[b] A list of all members of this Collaboration is given at the end of this issue.

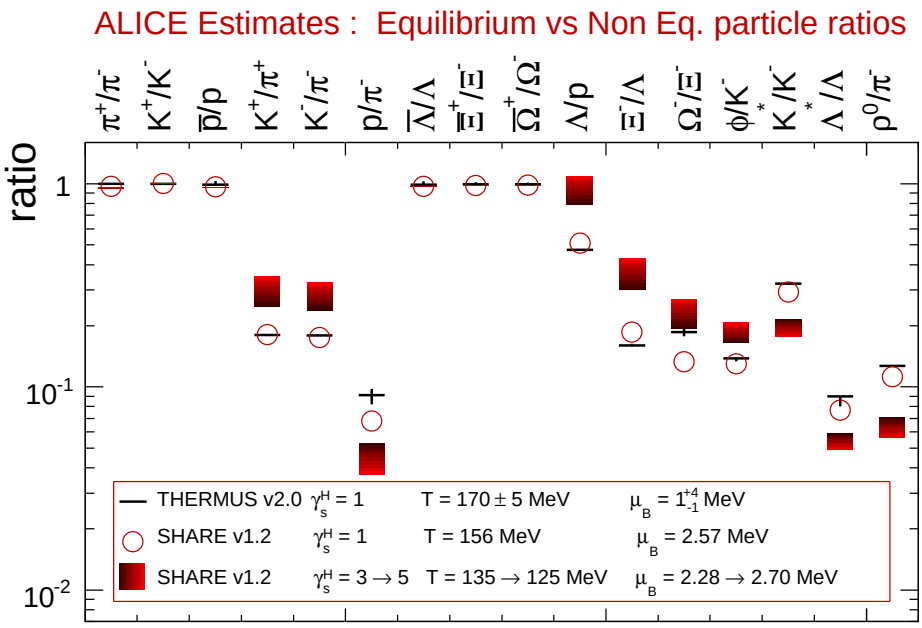

Fig. 1. Estimates of particle ratios in central Pb–Pb collisions at LHC energies for equilibrium (THERMUS [12]) and non equilibrium (SHARE [13]) statistical models with different assumptions related to chemical freeze-out conditions: i) for the equilibrium model, a chemical freeze-out temperature of T = 170 ± 5 MeV and a chemical potential $\mu_B = 1^{+4}_{-1}$ MeV were extrapolated from RHIC thermal fits [14]; ii) for the non equilibrium model, the strangeness equilibration is reflected in the strange quark phase space occupancy γ_s and the image of strangeness equilibrium in the deconfined source, $\gamma_s^{QGP} = 1$, results in an over-saturation $\gamma_s^H = 3 \rightarrow 5$ after sudden hadronization [15]. Strangeness saturation in the hadronic phase i.e. $\gamma_s^H = 1$ for the non equilibrium model is shown as a reference (open circles) and systematics comparison for the chemical freeze-out conditions (T = 156 MeV and $\mu_B \simeq 2.6$ MeV). Expected values for resonances are presented with no in-medium effects (see text).

For what is related to the overall strange quark production, most of the information is contained in the Wroblewski factor [10,11]:

$$\lambda_s \equiv 2\frac{\langle s\bar{s}\rangle}{\langle u\bar{u}\rangle + \langle d\bar{d}\rangle}$$

From RHIC to LHC energies, this factor should stay almost constant and reach $\simeq 0.43$ and $\simeq 0.20$ for respectively Pb–Pb and pp collisions [12].

In the same framework, many particle ratios can be estimated with T and μ_B where it is important to recall that ratios including (heavy) multi-strange baryons are sensitive to small variations of the temperature [16].

However the models may consider differently the degree of strangeness equilibration in the final state, which can be related to the QGP cooling under several assumptions. Figure 1 displays the estimates for particle ratios for two models. The equilibrium model (THERMUS) shown here assumes complete equilibrium of strangeness in the final (hadronic) state (γ_s^H=1) whereas for the non-equilibrium model (SHARE), equilibration for strange quarks in the QGP (γ_s^{QGP}=1) can lead to an over-saturation after sudden hadronization (γ_s^H=3 → 5). These two models are detailed in specific documents for their implementations and some of their results [12,13,14,15].

Within errors, THERMUS ratios correspond exactly to the former values of T and μ_B. Moreover, and as expected for a vanishing baryo-chemical potential, all anti-particle to particle ratios at LHC are shown to be unity. This was not yet the case at RHIC energies [17]. One can note that hadronic equilibrium ratios obtained with SHARE are similar although T differs significantly.

For non-identical species ratios, the differences between THERMUS and SHARE equilibrium results (lines vs. circles: mainly p/π^- and Ω^-/Ξ^-) can be interpreted as a systematical variation of the chemical temperature. On the contrary non-identical species ratios are very sensitive to the equilibrium hypothesis: significant deviations are observed especially where strange baryons are involved [16]. Particle ratios including resonances have to be taken cautiously. In-medium effects can be sizeable at the QGP stage (the lifetime of some resonances are of the order of, or even smaller than the one of the fireball) or later during the hadronic stage (e.g. rescattering and regeneration) [18]: these effects are not taken into account here.

From these comparisons and assuming that contributions from hard processes are marginal for these studies, the distinction between non-equilibrium and equilibrium scenarios should be within the reach of the ALICE experiment. Its dedicated particle identification capabilities are stated in the next section.

2.2 ALICE particle identification capabilities

The design of the ALICE experiment is ideal for particle identification (PID) in the soft physics sectors ($p_T <$ 2 GeV/c). Several detectors can be used for PID independently or simultaneously via, for instance, linear energy loss in gas detectors or silicon sensors, ring imaging Cherenkov or time of flight measurements [1]. Secondary vertex topology identification (for strange particle e.g. K^0_s, Λ or charged multi-strange ones e.g. Ξ and Ω) has the significant advantage to allow single PID over a wide range of p_T [19].

For a statistics of 10^7 central Pb–Pb collisions at top LHC energies, the identification ranges for particle spectra at mid-rapidity were estimated to be 0.2–12, 0.5–11, 1–8 and 1.5–7 GeV/c respectively for K^0_s, Λ, Ξ and Ω [19]. Transverse momentum spectra from pp collisions could be of similar ranges with a statistics of 10^9 events in one year of data taking [20].

3 Transverse momentum ratios for LHC collisions

In RHIC central heavy ion collisions, quark coalescence was suggested as a possible hadronization mechanism and explains qualitatively the mid-rapidity baryon/meson ratio at intermediate p_T. In pp collisions, such a hadronization scenario is not favoured due to the low phase space density in the final state.

In the following paragraphs, we will discuss coalescence mechanisms and predictions for Pb–Pb collisions at LHC. It will be shown that i) high baryon/meson ratios were also measured in elementary collisions for energies respectively 3 and 9 times the top RHIC ones; ii) a PYTHIA model [21] hardly reproduces such a behaviour even with the recent multiple parton interaction mechanisms and latest parton distribution functions (with higher gluon density at low Q^2).

3.1 Coalescence and baryon enhancement at intermediate transverse momentum

The intermediate p_T region can be defined between a soft domain, reproduced quite accurately by hydrodynamics, and an upper limit where the fragmentation of energetic partons dominates hadro-production. Constituent quark coalescence was suggested to be a hadronization mode in this region for describing hadron yields and spectra at RHIC by several models [22,23,24] with the possible inclusion of recombination between bulk and mini-jet quarks. Being a multi-parton process, recombination is closely related to the high phase space density available in heavy-ion collisions but obviously disfavoured in pp reactions.

Besides the magnitude of the elliptic flow, one major success of this picture is the description of the baryon over meson ratios as a function of p_T. At RHIC, it was quite surprising to see a kinematical region where the production of baryons exceeds the one of mesons with a similar flavour content [25,26]. From simple (constituent) quark counting considerations, the interplay of coalescence and fragmentation appears to explain the magnitude and almost the observed turnover of the $\bar{\mathrm{p}}/\pi^-$ and the Λ/K^0_S ratios [25].

For LHC energies, the turnover in the p/π^0 ratio was predicted to change slightly from $p_T = 3$ GeV/c to $\sim$ 4 GeV/c with uncertainties associated to the evolution of the transverse radial flow velocity [27].

3.2 Baryon over meson ratios in elementary collisions

For pp collisions at RHIC ($\sqrt{s} = 200$ GeV), the Λ/K^0_S ratio was also measured. A value of ~ 0.6 was obtained which is approximately one third of the value for central heavy-ion collisions [28].

However, the UA1 and CDF Collaborations measured the $(\Lambda + \bar{\Lambda})$ and K^0_S spectra at mid-rapidity in minimum bias $\mathrm{p} + \bar{\mathrm{p}}$ collisions at the higher energies of respectively $\sqrt{s} = 630$ GeV [29] and 1800 GeV [30]. If one computes the $(\Lambda + \bar{\Lambda})/\mathrm{K}^0_S$ ratio from the fit parameterizations they reported, the observed magnitude is closer to the RHIC heavy-ion one, although coalescence mechanisms are difficult to invoke here. These ratios are shown in Fig. 2.

3.3 PYTHIA simulations and extrapolations

Since the coalescence mechanism originates from the hypothesis of multi-parton processes, it sounds legitimate to investigate this path for LHC pp collisions at the top energy of $\sqrt{s} = 14$ TeV. The PYTHIA model offers such a possibility to include multiple parton interactions [31].

The first difficulty is the extrapolation from Tevatron to LHC energies. The PYTHIA *configuration 1* is proposed by the ATLAS Collaboration [32] and based on the CTEQ5 parton density functions (PDF) [33], PYTHIA version 6.2 and Tevatron Rick Field's tune A [34]. It is compared here to the *configuration 2* set by the "Les Houches Working Group" (LHWG) [35].

Major modifications were performed from the version 6.2 to 6.3 of PYTHIA. One of these is the new treatment of multiple parton interactions which is supposed to lead to a better underlying event description [31]. The LHWG based their extrapolation on this latest implementation and the CTEQ6 PDF which has a higher gluon density function at low Q^2 than CTEQ5 [35]. It is worth mentioning that for these simulations, anti-particle to particle ratios such as $\bar{\mathrm{p}}/\mathrm{p}$ and $\bar{\Lambda}/\Lambda$ were checked to be flat in the p_T range presented in Figure 2. Therefore no hard scattering effects from valence quarks are hidden in the addition of the Λ and the $\bar{\Lambda}$ spectra. This sum was only performed here for having a better statistics and for consistency with UA1 and CDF data discussed in section 3.2.

The $(\Lambda+\bar{\Lambda})/\mathrm{K}^0_s$ ratios obtained for both configurations and 1 M minimum bias pp collisions at $\sqrt{s} = 14$ TeV are displayed on Figure 2 together with UA1 and CDF data. For the *configuration 1*, the ratio increases up to $p_T =$ 4 GeV/c and then flattens at ~ 0.4. In the *configuration*

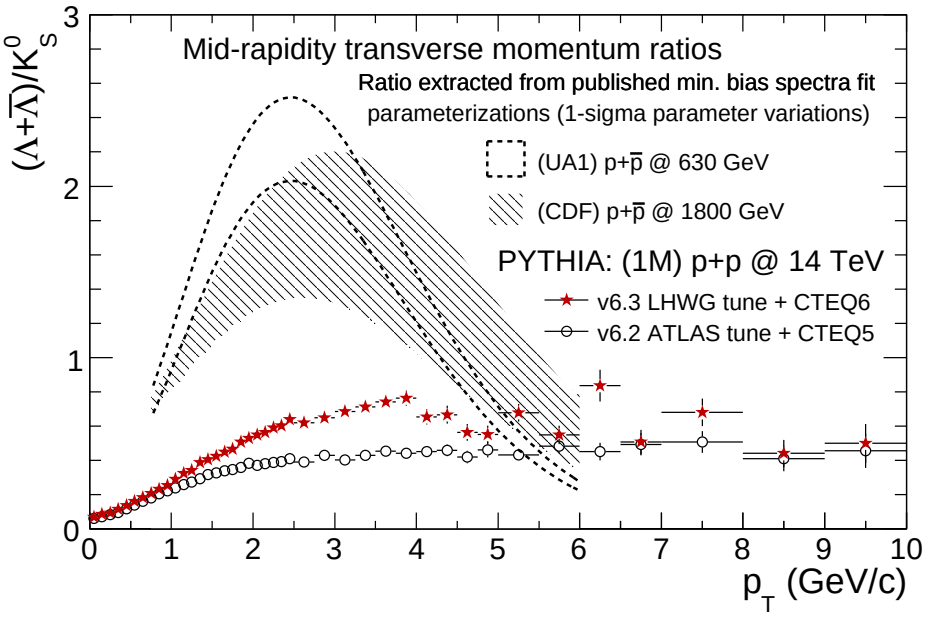

Fig. 2. Baryon over meson transverse momentum ratios for single strange particles $(\Lambda+\bar{\Lambda})/\mathrm{K}^0_s$ at mid-rapidity for minimum bias elementary collisions. For $\mathrm{p}+\bar{\mathrm{p}}$ results at $\sqrt{s} = 630$ GeV (UA1 Collaboration) [29] and $\sqrt{s} = 1800$ GeV (CDF Collaboration) [30], the measured ratios are presented as areas where the published fit parameterizations were used for the spectra (allowing 1-σ error for each parameter). Ratios extracted from PYTHIA simulations are shown for 1M simulated $\mathrm{p}+\mathrm{p}$ minimum bias events at LHC top energies i.e. $\sqrt{s} = 14$ TeV. Errors are statistical only. Further details and references for these simulations can be found in the text.

2, a clear increase is observed, reaching ~ 0.7 at $p_T = 4$ GeV/c and showing that the cumulated effects of the higher gluon density at low Q^2 and the multiple parton interactions give qualitatively the expected behaviour.

4 Conclusion

Particle yields and transverse momentum spectra or ratios including the strange flavor will be part of the first ALICE results. These measurements will benefit from the particle identification capability of the experiment in the soft sector up to the limit where the fragmentation of energetic partons dominates hadro-production. We expect that discrimination between non-equilibrium and equilibrium scenarios in heavy-ion collisions will be possible and that a better characterization of baryon production in pp collisions will help defining the underlying event structure.

References

1. F Carminati *et al.*, J. Phys. **G30**, (2004) 1517.
2. J. Letessier and J. Rafelski, nucl-th/0504028.
3. J. Speltz, J. Phys. **G31**, (2005) S1025.
4. J. Adams *et al.*, Nucl. Phys. **A757**, (2005) 102.
5. K. Adcox *et al.*, Nucl. Phys. **A757**, (2005) 184.
6. F. Becattini *et al.*, Phys. Rev. **C654**, (2001) 024901.
7. A. Andronic, P. Braun-Munzinger and J. Stachel, Nucl. Phys. **A772** (2006) 167.
8. J. Cleymans and K. Redlich, Phys. Rev. Lett. **81**, (1998) 5284.
9. J. Cleymans *et al.*, hep-ph/0607164.
10. A. Wroblewski, Acta. Phys. Polon. **B16**, (1985) 379.
11. V.V. Anisovich and M.N. Kobrinsky, Phys. Lett. **B52**, (1974) 217.
12. S. Wheaton and J. Cleymans, hep-ph/0407174.
13. G. Torrieri *et al.*, Comput. Phys. Commun. **167** (2005) 229 and nucl-th/0603026.
14. J. Cleymans *et al.*, Phys. Rev. **C71**, (2005) 054901.
15. J. Rafelski and J. Letessier, Eur. Phys. J **C45**, (2006) 61.
16. J. Cleymans *et al.*, hep-ph/0604237.
17. B. Hippolyte, nucl-ex/0306017.
18. J. Adams *et al.*, Phys. Rev. Lett. **92**, (2004) 092301, Phys. Rev. **C71**, (2005) 064902 and nucl-ex/0604019.
19. R. Vernet *et al.* ALICE Internal Note (2005-042).
20. L. Gaudichet, ALICE Internal Note (2005-041).
21. T. Sjöstrand *et al.*, Comput. Phys. Commun. **82**, (1994) 74 and hep-ph/0308153.
22. R.J. Fries *et al.* Phys. Rev. **C68** 044902 (2003).
23. V. Greco, C.M. Ko and P. Lèvai, Phys. Rev. **C68**, (2003) 034904 and Phys. Rev. Lett. **90**, (2003) 202302.
24. R.C. Hwa and C.B. Yang, Phys. Rev. **C67**, (2003) 034902.
25. J. Adams *et al.*, nucl-ex/0601042 and nucl-ex/0606003.
26. S.S. Adler *et al*, Phys. Rev. **C69**, (2004) 034909.
27. R.J. Fries and B. Müller, Eur. Phys. J **C34**, (2004) S279.
28. M.A.C. Lamont, J. Phys. **G30**, (2004) S963.
29. G. Bocquet *et al*, Phys. Lett. **B366**, (1996) 441.
30. D. Acosta *et al*, Phys. Rev. **D72**, (2005) 052001.
31. T. Sjostrand and P. Skands, Eur. Phys. J **C39**, (2005) 129.
32. A. Moraes *et al.* ATL-PHYS-PUB-2005-007.
33. J. Pumplin *et al.*, JHEP **0207**, (2002) 012.

34. R. Field, talk at ME/MC Tuning Workshop (2002), Fermilab.
35. C. Buttar *et al.*, hep-ph/0604120.